Draft version November 6, 2020
Preprint typeset using LaTeX style emulateapj v. 01/23/15

THE CLUSTERS HIDING IN PLAIN SIGHT (*CHiPS*) SURVEY: CHIPS1911+4455 (PHOENIX MEETS EL GORDO)

Taweewat Somboonpanyakul[1], Michael McDonald[1], Matthew Bayliss[2], Mark Voit[3], Megan Donahue[3], Massimo Gaspari[4,5], Håkon Dahle[6], Emil Rivera-Thorsen[6], and Antony Stark[7]

Draft version November 6, 2020

ABSTRACT

We present high resolution optical images from the *Hubble* Space Telescope, X-ray images from the *Chandra* X-ray Observatory, and optical spectra from the Nordic Optical Telescope for the newly-discovered galaxy cluster, CHIPS1911+4455 at $z = 0.485$. CHIPS1911+4455 was discovered in the Clusters Hiding in Plain Sight (*CHiPS*) survey, which sought to discover galaxy clusters with extreme central galaxies that were misidentified as isolated X-ray point sources in the ROSAT All-Sky Survey. With new *Chandra* X-ray observations, we determine the core density (∼10 kpc) to be 0.0884 cm^{-3} and the core entropy to be 17^{+2}_{-9} keVcm^2, suggesting a strong cool core, which are typically found at the centers of relaxed clusters. However, the large-scale morphology of CHIPS1911+4455 is highly asymmetric, pointing to a more dynamically active and turbulent cluster. Furthermore, the *Hubble* images reveal a massive, filamentary starburst near the brightest cluster galaxy (BCG). We measure the star formation rate for the BCG to be 140–190 $M_\odot\,yr^{-1}$, which is one of the highest rates measured in a central cluster galaxy to date. One possible scenario for CHIPS1911+4455 is that the cool core was displaced during a major merger and rapidly cooled, with cool, star-forming gas raining back toward the core. This unique system is an excellent case study for high-redshift clusters, where such phenomena are proving to be more common. Further studies of such systems will drastically improve our understanding of the relation between cluster mergers and cooling, and how these fit in the bigger picture of active galactic nuclei (AGN) feedback.

Subject headings: galaxies: clusters: general — galaxies: clusters: intracluster medium — X-rays: galaxies: clusters

1. INTRODUCTION

Early X-ray observations of the intracluster medium (ICM) in the center of galaxy clusters revealed cooling times much shorter than the Hubble time, which led to the development of the cooling flow model (e.g., Fabian 1994). In this model, hot gas in dense cores should have radiatively cooled and fueled 100–1000 $M_\odot\,yr^{-1}$ starbursts in the central brightest cluster galaxies (BCGs). However, many studies have shown that BCGs are only forming stars at ∼1% of this rate (e.g., McDonald et al. 2018). A promising mechanism proposed for preventing cooling of the ICM is AGN heating by jets and bubble-induced weak shocks (see reviews by Fabian 2012; McNamara & Nulsen 2012; Gaspari et al. 2020). Evidence supporting these theories includes the ubiquitous presence of radio galaxies at the center of clusters (Sun 2009) and the similarity between the mechanical energy released by AGN driven bubbles and the energy needed to quench cooling (e.g. Rafferty et al. 2008; Birzan et al. 2008; Hlavacek-Larrondo et al. 2015).

Galaxy clusters with signatures of cooling in their centers are often called "cool-core" (CC) clusters, with their counterparts being referred to as "non cool-core" (NCC) clusters. Hudson et al. (2010) found that the best way to segregate the two is to consider their central cooling time (t_{cool}). Specifically, CC clusters have $t_{cool} < 7.7$ Gyr, while clusters with $t_{cool} < 1.0$ Gyr are referred to as "strong CCs". A number of observational studies have found that CCs are mostly found in relaxed clusters while NCCs reside in dynamically-active clusters. Indeed, all of the strongest CCs known (based on the classical cooling rate) are found in the most relaxed clusters (e.g., Phoenix (McDonald et al. 2012), Abell 1835 (McNamara et al. 2006), Zw3146 (Edge et al. 1994)). This is also consistent with a variety of other students that found star-forming BCGs in the most relaxed CC clusters (Crawford et al. 1999; Donahue et al. 2010; Molendi et al. 2016),. On the other hand, morphologically-disturbed clusters (which are likely to be recent mergers) generally have no evidence for ongoing cooling – the poster child for such clusters is the extremely massive El Gordo cluster (Menanteau et al. 2012). Major mergers have the potential to destroy cool cores (Burns et al. 2008; Poole et al. 2008) through shock-heating (Burns et al. 1997) and mixing (Gómez et al. 2002).

The discovery of CHIPS1911+4455 (Somboonpanyakul et al., in press) runs counter to these established norms, since it not only harbors a very blue (star-

[1] Kavli Institute for Astrophysics and Space Research, Massachusetts Institute of Technology, 77 Massachusetts Avenue, Cambridge, MA 02139
[2] Department of Physics, University of Cincinnati, Cincinnati, OH 45221, USA
[4] INAF, Osservatorio di Astrofisica e Scienza dello Spazio, via P. Gobetti 93/3, 40129 Bologna, Italy
[5] Department of Astrophysical Sciences, Princeton University, Princeton, NJ 08544, USA
[6] Institute of Theoretical Astrophysics, University of Oslo, P.O. Box 1029, Blindern, NO-0315 Oslo, Norway
[7] Harvard-Smithsonian Center for Astrophysics, 60 Garden St., Cambridge MA 02138, USA
[3] Physics & Astronomy Department, Michigan State University, East Lansing, MI 48824-2320, USA

forming) galaxy in the center, but also shows a highly-disturbed morphology on both large (∼200 kpc) and small (∼20 kpc) scales. There are no known nearby clusters that have properties similar to CHIP1911+4455, though McDonald et al. (2016) reports a higher fraction of star-forming BCGs in merging clusters at $z > 1$. This implies that CHIPS1911+4455 may provide an avenue for studying a high-redshift phenomenon in a low-redshift cluster. To fully understand this system we have obtain new observations in the core of CHIPS1911+4455, which we will discuss below.

Throughout this paper, we assume $H_0 = 70\,\mathrm{km\,s^{-1}Mpc^{-1}}$, $\Omega_m = 0.3$, and $\Omega_\Lambda = 0.7$. All errors are $1\,\sigma$ unless noted otherwise.

2. OBSERVATIONS

In this section, we summarize the acquisition and reduction of data obtained from the *Chandra* X-ray telescope, the *Hubble* Space Telescope and the Nordic Optical Telescope (NOT).

2.1. *X-ray: Chandra*

CHIPS1911+4455 (OBSID: 21544) was observed in 2019 with *Chandra* ACIS-I for a total of 30.5 ks. The data were analyzed with `CIAO` v4.11 and `CALDB` v4.8.5. It was recalibrated with VFAINT mode for improved background screening. In order to look for small-scale structures near the center of the cluster, images were smoothed adaptively, using `CSMOOTH`[8] which smooths images on variable scales to achieve a uniform signal-to-noise ratio over the full image, as shown in the left panel of Fig. 1.

The temperature profile was extracted from coarse annuli so that the number of counts per annulus was around 800, which is enough to get well-constrained temperature measurements (ΔkT/kT ∼20%). All spectra were fit simultaneously with the `APEC` model for the cluster emission and the Milky Way ($kT = 0.18\,\mathrm{keV}$), the `PHABS` model for Galactic absorption, and the `BREMSS` model to represent a hard background ($kT = 0.18\,\mathrm{keV}$) from unresolved point sources, following McDonald et al. (2013). The *WSTAT* statistic was used.

The gas density profile was created by first computing the 0.7-2.0 keV surface brightness profile. The conversion from the X-ray surface brightness profile to the emission-measure profile ($\mathrm{EM}(r) = \int n_p n_e dl$) was calculated as a function of radius based on the best-fit temperature profile and assuming a collisionally-ionized plasma `APEC` model with metallicity $0.3\mathrm{Z}_\odot$. For more details of the X-ray analysis, see Somboonpanyakul et al. (2018).

2.2. *Optical: Hubble*

CHIPS1911+4455 was observed for two orbits with the *Hubble* Space Telescope (HST) during Cycle 27. The data include medium band F550M data from the Advance Camera for Surveys (ACS) and broad band F110W data from the and Wide Field Camera infrared channel (WFC3-IR). The F550M filter contains both the blue continuum and the bright [O II] doublet at the redshift of the cluster, which should both be elevated in star-forming regions. The F110W filter, on the other hand, is sensitive to the red continuum, probing the old stellar populations of the BCG and other cluster members.

[8] https://cxc.harvard.edu/ciao/ahelp/csmooth.html

2.3. *Optical Spectra: Nordic Telescope*

Two optical spectra of the BCG of CHIPS1911+4455 were obtained with the Alhambra Faint Object Spectrograph and Camera (ALFOSC) at the 2.56m Nordic Optical Telescope (NOT) on May 9th, 2019. One of the spectra was obtained from Grism#4 (R=360, 3200–9600Å) with 1.3″ slit for 1500-second exposure. The other spectrum was a stack of two 1100-second spectra from Grism#5 (R=415, 5000–10700Å) with 1.3″ slit at 90° from the first spectrum. Wavelength solutions for the two spectra were calibrated with HeNe and ThAr arc lamps, respectively. Masks were applied to remove cosmic-rays before the 1D spectra were extracted from the 2D spectral images. The 1D spectra were then normalized from off-source regions surrounding the 1D extraction region.

3. RESULTS

3.1. *CHIPS1911+4455: A Strong Cool Core*

The left panel of Fig. 2 shows the X-ray EM profile of CHIPS1911+4455 out to ∼1000 kpc. The inner core density at 10 kpc is $0.0884\,\mathrm{cm^{-3}}$, which is among the highest measured to date (McDonald et al. 2017). Meanwhile, the temperature profile in the middle panel of Fig. 2 also exhibits a temperature gradient from 4 keV at ∼10 kpc to a maximum of ∼8 keV at ∼300 kpc.

The entropy of the ICM ($K \equiv kTn_e^{-2/3}$) reflects the thermal history of a cluster, which is solely affected by heat gains and losses (Cavagnolo et al. 2009; Panagoulia et al. 2014), while the cooling time ($t_{cool} \equiv \frac{3}{2}\frac{(n_e+n_p)kT}{n_e n_p \Lambda(T)}$) represents the amount of time required for the ICM to radiate all the excess heat. The right panel of Fig. 2 shows the cooling time profile of CHIPS1911+4455. The central cooling time at 10 kpc is $98^{+7}_{-32}\,\mathrm{Myr}$, which is classified as a strong cool core (Hudson et al. 2010). The non-projected entropy profiles for CHIPS1911+4455, the Phoenix cluster, and hundreds of clusters from the ACCEPT survey (Cavagnolo et al. 2009) are shown in Fig. 3. Both CHIPS1911+4455 and the Phoenix cluster have entropy profiles that are among the lowest known. The core entropy (at 10 kpc) for CHIPS1911+4455 is $17^{+2}_{-9}\,\mathrm{keVcm^2}$, which is in the 5^{th} percentile of all clusters in the ACCEPT survey.

3.2. *CHIPS1911+4455: A Major Merger*

There are various ways to define morphology with X-ray data. The two particular quantities we consider are the sharpness of the peak in the surface brightness profile (peakiness) and the distance between the center of symmetry on small and large scale (symmetry), following Mantz et al. (2015). The peakiness measure is a proxy for the presence of a cool core, which are typically found in relaxed clusters. On the other hand, a cluster with high symmetry implies that a cluster appears similar on small and large scales, which is also evidence that the cluster is dynamically relaxed. Given

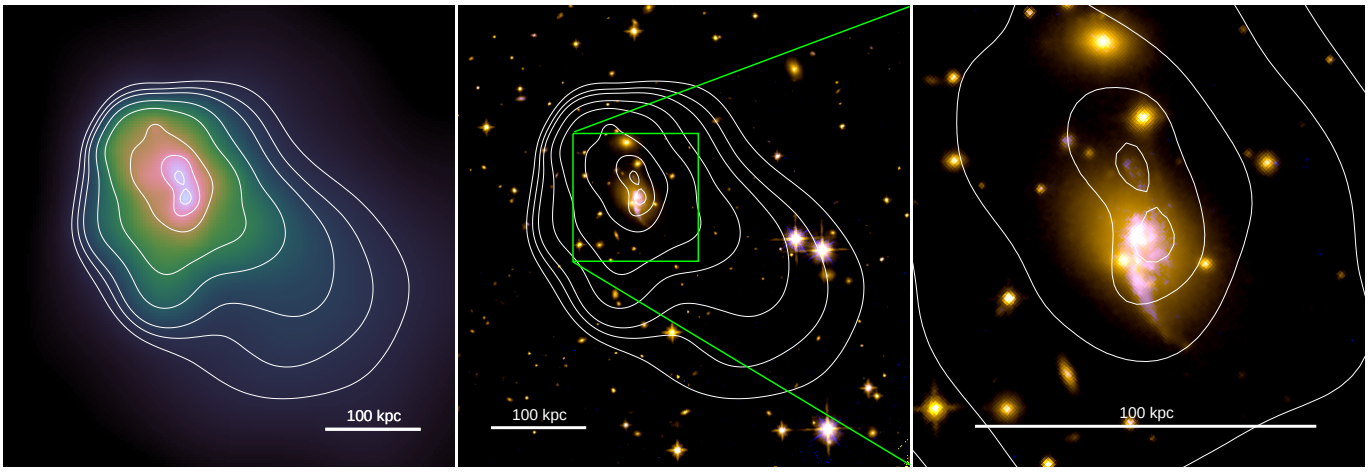

FIG. 1.— Left: *Chandra* 0.5-7.0 keV image of CHIPS1911+4455, highlighting the asymmetric morphology on both small and large scales. Middle: The *Hubble* images with an overlay of the X-ray contour on top. The contour lines were chosen to guide the eyes. Right: The *Hubble* images of the central galaxy, showing the blue star-forming filaments, extending on scales of $\sim$ 30 kpc. These images show the direction of the extended hot gas in relation to the direction of the blue complex filaments, suggesting that the two might be connecting together.

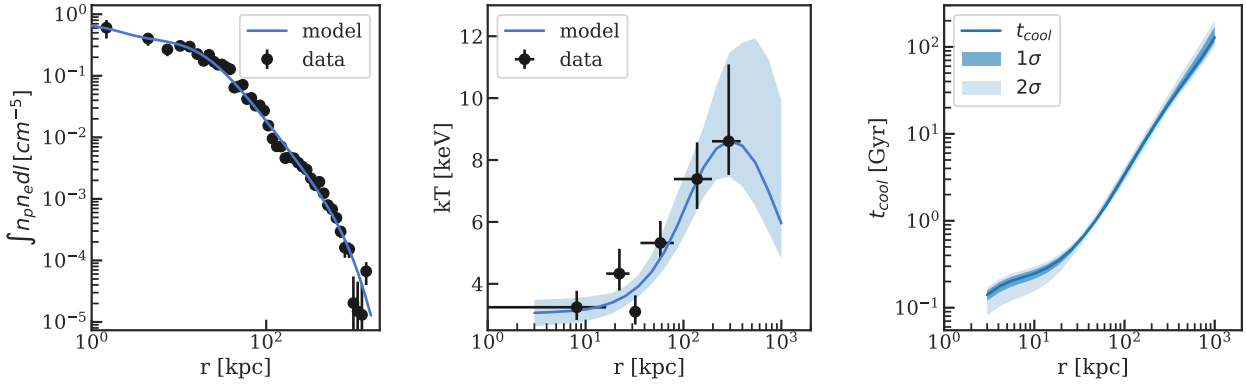

FIG. 2.— Left: The surface brightness profile of CHIPS1911+4455. The black dots are data points, and the blue line is the best-fit model (see Somboonpanyakul et al. 2018, for a further description of this modeling). Middle: the projected 2-D temperature profile of the cluster. The black dots are data extracted from modeling of the X-ray spectra. The blue line is the best-fit model following Vikhlinin et al. (2006). Right: The cooling time profile of the cluster. The cyan-shaded region corresponds to 1σ credible region from the models in the left and center panels, while the light blue-shaded region corresponds to 2σ credible region. This cluster is classified as a strong cool core, based on a large drop in the core temperature and a central cooling time less than 1 Gyr (Hudson et al. 2010).

that both of these proxies probe the dynamical state of the cluster, albeit in different ways, it is unsurprising that they are correlated Mantz et al. (2015). The green points in Fig. 4 show the population of relaxed clusters in this morphology plane. For CHIPS1911+4455, the peakiness is measured to be -0.501, which is in the 96$^{\rm th}$ percentile of all clusters in Mantz et al. (2015)'s sample. Yet, the symmetry is estimated to be 0.425, which is in the 93$^{\rm rd}$ percentile for disturbed clusters. The fact that CHIPS1911+4455 is simultaneously one of the strongest cool cores *and* most asymmetric clusters known is highly unusual.

3.3. *CHIPS1911+4455: A Starburst BCG*

In the two rightmost panels of Fig. 1, we compare optical images from *Hubble* with the X-ray contours from *Chandra*. The *Hubble* images show that the red emission from the old stellar populations are relatively smooth and symmetric, while the blue emission from the young stellar populations and cool gas is clumpy, asymmetric, and extended on >30 kpc scales. Since the direction of the extended blue emission is not in the direction of any nearby galaxy, it is possible that the young stars are forming directly from the cooling ICM. The filamentary complex structures in the blue emission are similar to the emission nebula in the Phoenix cluster (McDonald et al. 2019) and other nearby cool core clusters (e.g., McDonald et al. 2011; Tremblay et al. 2015).

From the 1D optical spectra in Fig. 5, we identify several bright emission lines, including Hβ and the [O II] doublet. The relative lack of bright [O III] lines compared to [O II] indicates that the central galaxy in CHIPS1911+4455 is a massive starburst and not a bright AGN. From the two spectra, we measure the [O II] equivalent width to be 40.9 ± 1.0 Å and 41.2 ± 1.0 Å, which are consistent with each other. To convert to flux,

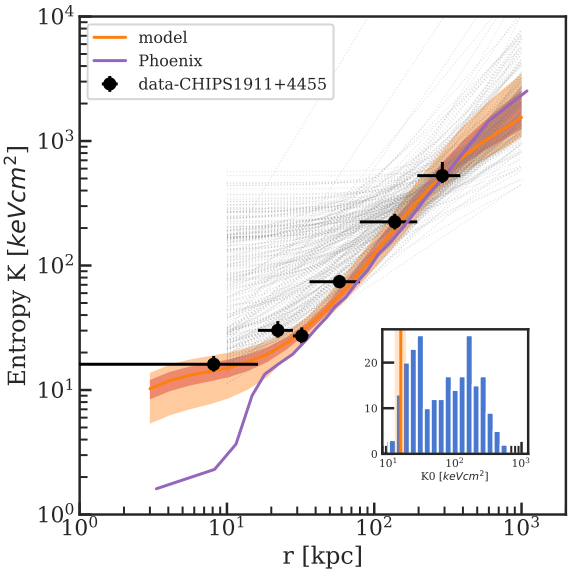

FIG. 3.— Entropy profile for CHIPS1911+4455 (orange), compared to 239 clusters from the ACCEPT survey (gray; Cavagnolo et al. 2009) and the Phoenix cluster (purple; McDonald et al. 2019). The shaded region corresponds to 1σ and 2σ credible region (see Figure 2). The black dots are data points, estimated from the projected 2D temperature data and the 3D density model. The inset shows the histogram of the core entropy ($r < 10$ kpc) of all the ACCEPT clusters and CHIPS1911+4455 (orange). CHIPS1911+4455's core entropy is in the lowest 10% of all ACCEPT clusters.

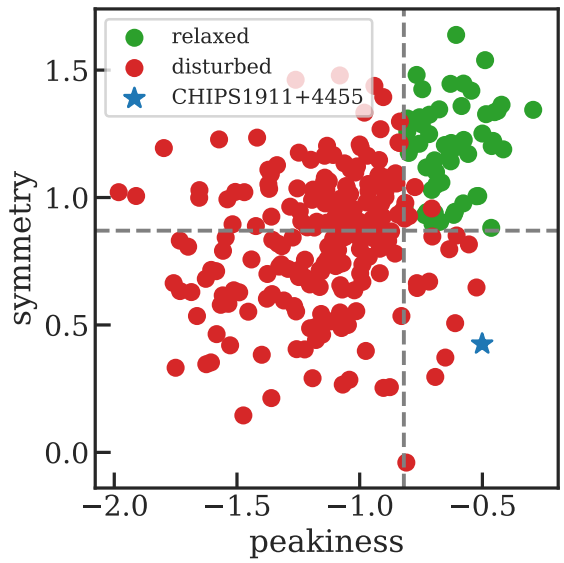

FIG. 4.— Distribution of X-ray symmetry and peakiness for clusters presented in Mantz et al. (2015). Dashed lines show the cuts used to define the relaxed sample, which is shown in green, while red points show unrelaxed clusters. The blue star represents the location of CHIPS1911+4455, which is the peakiest cluster with large-scale asymmetry.

the spectral energy distribution (SED) of the galaxy is generated based on data from Pan-STARRS (g, i, r, z, and y) (Tonry et al. 2012) and from WISE ($w1$ and $w2$) (Wright et al. 2010). We modeled the SED with a linear combination of "young" and "old" stellar populations, along with dust reddening (Calzetti et al. 2000). The best-fit SED model is shown in the right panel of Fig. 5. From the SED fit, the de-reddened continuum flux at the location of [O II]is $3.5 \pm 0.5 \times 10^{-16}$ erg s^{-1} cm^{-2} Å^{-1}. The continuum flux is multiplied with the EW to obtain the [O II] line flux. We then estimate the SFR of the central galaxy to be 189^{+25}_{-22} M$_\odot$ yr^{-1}, based on Kennicutt (1998).

Another way to measure SFR is to use the $24\mu m$ emission since mid-IR fluxes are unaffected by dust extinction, unlike UV and optical tracers. Instead, mid-IR emission comes from the reprocessed light by dust, produced from recently formed stars. Based on the WISE4 flux ($\sim 4\times10^{-18}$ erg s^{-1} cm^{-2} Å^{-1}), we estimate the SFR for the central galaxy to be 143^{+31}_{-26}, M$_\odot$ yr^{-1}, using the SFR calibration from Cluver et al. (2017).

Considering both the [O II] emission line luminosity and the mid-IR continuum, we obtain consistent SFRs of ∼140–190 M$_\odot$ yr^{-1}, making the BCG in CHIPS1911+4455 the one of the most star-forming BCGs in the $z < 1$ Universe (see e.g., McDonald et al. 2018)

4. DISCUSSION

Based on Sections 3.1–3.3, CHIPS1911+445 is a unique system in the nearby universe ($z < 0.5$) with a large star formation rate in the BCG and a strong cool core, even though its large-scale morphology is more similar to a recent merger. It is common knowledge that at low-redshift, the most star-forming BCGs tend to be located in the most relaxed, cool-core clusters (Cavagnolo et al. 2008; Donahue et al. 2010) (e.g., Abell 1835 and the Phoenix cluster). Whereas, the star formation rate in high-redshift BCGs tend to be higher in dynamically active, non cool-core clusters (McDonald et al. 2016; Bonaventura et al. 2017). CHIPS1911+4455 may represent a low-redshift analog of these high redshift systems, allowing us to study physical processes that may have been much more common at early times. Further studies of CHIPS1911+4455 may allow us to understand more about these distant starburst BCGs, which are much more difficult to study with our current technologies and instruments.

In the precipitation scenario for regulating star formation in galaxy clusters, cool clouds condense and can form stars when $t_{\rm cool}/t_{\rm ff} < 10$ where $t_{\rm cool}$ is the cooling time for the local gas and $t_{\rm ff}$ is the free fall time (e.g., Voit et al. 2015; Gaspari et al. 2020). The threshold of 10 can move depending on a medium's susceptibility to condensation, the slope of the entropy profile, the amount of turbulence, and the amplitude of entropy perturbation (Voit et al. 2017; Voit 2018). There are two ways to cross this threshold: by decreasing $t_{\rm cool}$ or increasing $t_{\rm ff}$. If a dense cool core is physically displaced from the center of the gravitational potential well, $t_{\rm ff}$ would be higher at the new location, making it easier for the gas to condense on timescales faster than the free fall time, and eventually form stars. This scenario would not immediately trigger

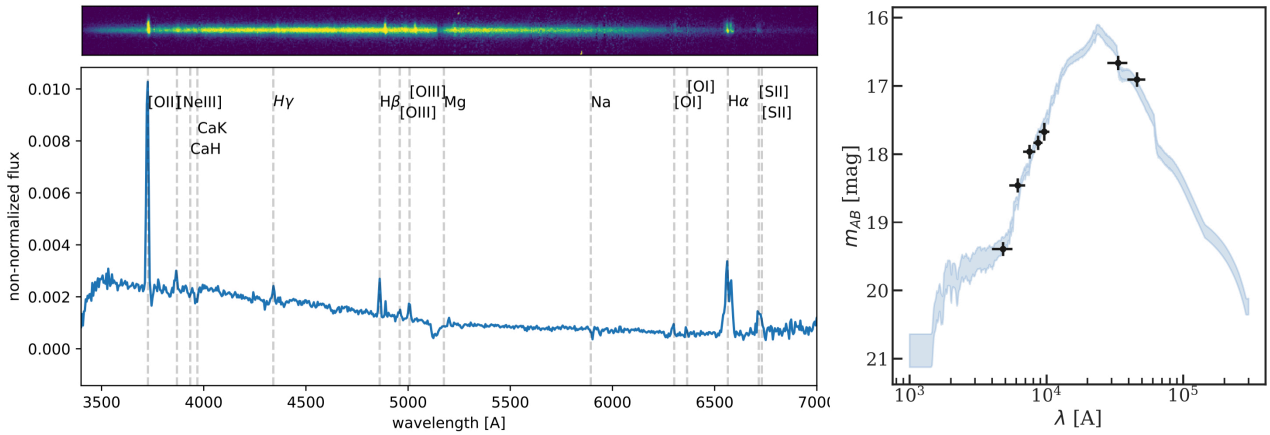

FIG. 5.— Top left: The 2D spectral image of the BCG of CHIPS1911+4455 from the Nordic Optical Telescope showing that the line-emitting gas is extended along the slit (vertical) direction. Bottom left: The 1D spectrum in the rest frame from the 2D spectral image above. Grey dash lines show the location of well-known emission lines. The spectrum clearly shows the strong [O II] doublet at 3727 Å and the Hα emission line at 6562.8 Å. Right: The fitted spectral energy distribution (SED) model with broad-band optical data (g, r, i, z, and y) from Pan-STARRS and mid-IR from WISE.

AGN feedback, due to the offset between the cooling and the central black hole, allowing for a potential short-term break in the feedback cycle. One possible mechanism to displace a cool core from the center is an interaction with another group or cluster via a merger. This may explain what has happened to CHIPS1911+4455: the high SFR is a result of low-entropy gas being displaced from the central AGN by bulk motions induced by a major merger. This system provides evidence that cluster mergers can, in fact, stimulate star formation and enhance cooling, especially in the distant universe when mergers were more common compared to present time (Fakhouri et al. 2010). Closely related to this, in the chaotic cold accretion scenario (CCA; e.g., Gaspari et al. 2019) turbulence is a key ingredient to drive direct non-linear thermal instability and extended condensation. During CCA the global driver can be tied not only to AGN feedback, but to mergers too, which can stimulate significant amount of turbulence (e.g., Lau et al. 2017) and density fluctuations at large injection scales, enabling enhanced condensation.

Looking closely at the X-ray image in Fig 1, we see a disturbed cool core or even two distinct cool cores. When we match the locations of the two possible cool cores with the *Hubble* images, only the southern one has a galaxy counterpart while the northern one does not correspond to any particular galaxy. This suggests that the northern cool core might be dense gas that is dislodged from the southern cool core which remains at the location of the BCG. In addition, the blue complex filaments in the *Hubble* images are extended in the same direction toward the northern cool core. In fact, the northern cool core coincides with a blue clump in the northern direction of the optical images, suggesting that the shifted dense gas cools at the new location as it falls back toward the center.

5. CONCLUSION

In this work, we present new data from *Hubble*, *Chandra*, and the Nordic Optical Telescope. Our findings are summarized as follows:

1. We measure the ICM density in the core ($r < 10\,\mathrm{kpc}$) of CHIPS1911+4455 to be 0.09 cm^{-3}, which is typical for a cool-core cluster. The core entropy is 17^{+2}_{-9} keV cm^2, which is within the lowest ten percent for cluster cores from the ACCEPT samples (Cavagnolo et al. 2009). The low entropy core is a clear signature of strong cooling in the center of the cluster.

2. The X-ray morphology of CHIPS1911+4455 is highly peaked in the center (96th percentile) and very asymmetric (93rd percentile) compared to a large sample of X-ray-selected clusters. This contradiction in its morphology between a relaxed (peaky) cluster and a dynamically active (asymmetric) cluster is highly unusual, and is rarely observed.

3. Based on the [O II] emission line luminosity, we measure a SFR in the BCG of $189^{+25}_{-22}\,\mathrm{M}_\odot\,\mathrm{yr}^{-1}$. This is consistent with an estimate based on the mid-IR continuum of $143^{+31}_{-26}\,\mathrm{M}_\odot\,\mathrm{yr}^{-1}$. This BCG is among the five most star-forming BCGs in the low-z Universe.

4. The *Hubble* images show complex blue filaments near the BCG, confirming the presence of a massive starburst. In addition, these data show no evidence for an ongoing merger, suggesting that the observed star formation is fueled by cooling of the hot ICM.

5. Rapid cooling in this system may have been triggered by a dynamical interaction between two similar-mass clusters. In this scenario, some of the low-entropy gas from the more massive cluster is dragged away from the center, where cooling is more favorable due to the longer mixing times, enhanced large-scale turbulence and CCA rain, and lack of a central AGN. This system may provide a link to high-redshift clusters, where previous studies have found an abundance of star-forming BCGs in dynamically-active clusters.

CHIPS1911+4455 is the first low-redshift ($z < 1$) galaxy cluster with this distinctive characteristic (hosting a high star-forming BCG and a strong cool-core but having a disturbed morphology). The cluster was discovered by the Clusters Hiding in Plain Sight (*CHiPS*) survey because of its exceptionally bright cool core that appears to be point-like in previous X-ray cluster catalogs (Somboonpanyakul et al. 2018). CHIPS1911+4455 represents a unique opportunity to understand the relationship between a merging galaxy cluster and star formation in its BCG, which, in turn, unravels an alternative method to form cooling flows and massive starbursts apart from a simple accretion model. This mechanism will become much more important at high redshift ($z > 1$) when the cluster merger rate is significantly higher (Fakhouri et al. 2010; McDonald et al. 2016).

ACKNOWLEDGEMENTS

T. S. and M. M. acknowledge support from the Kavli Research Investment Fund at MIT, Chandra Award Number GO9-20116X, and by Hubble Award Number HST-GO-16038. M. G. acknowledges partial support by NASA Chandra GO8-19104X/GO9-20114X and HST GO-15890.020-A. H. D. and E. R.T. acknowledge support from the Research Council of Norway.

REFERENCES

Bîrzan, L., McNamara, B. R., Nulsen, P. E. J., et al. 2008, ApJ, 686, 859
Bonaventura, N. R., Webb, T. M. A., Muzzin, A., et al. 2017, MNRAS, 469, 1259
Burns, J. O., Loken, C., Gomez, P., et al. 1997, Galactic Cluster Cooling Flows, 21
Burns, J. O., Hallman, E. J., Gantner, B., et al. 2008, ApJ, 675, 1125
Calzetti, D., Armus, L., Bohlin, R. C., et al. 2000, ApJ, 533, 682
Cavagnolo, K. W., Donahue, M., Voit, G. M., et al. 2008, ApJ, 683, L107
Cavagnolo, K. W., Donahue, M., Voit, G. M., et al. 2009, ApJS, 182, 12
Cluver, M. E., Jarrett, T. H., Dale, D. A., et al. 2017, ApJ, 850, 68
Crawford, C. S., Allen, S. W., Ebeling, H., et al. 1999, MNRAS, 306, 857
Donahue, M., Bruch, S., Wang, E., et al. 2010, ApJ, 715, 881
Edge, A. C., Fabian, A. C., Allen, S. W., et al. 1994, MNRAS, 270, L1
Fabian, A. C. 1994, ARA&A, 32, 277
Fabian, A. C. 2012, ARA&A, 50, 455
Fakhouri, O., Ma, C.-P., & Boylan-Kolchin, M. 2010, MNRAS, 406, 2267
Gaspari, M., Eckert, D., Ettori, S., et al. 2019, ApJ, 884, 169.
Gaspari, M., Tombesi, F., & Cappi, M. 2020, Nature Astronomy, 4, 10.
Gómez, P. L., Loken, C., Roettiger, K., et al. 2002, ApJ, 569, 122
Hlavacek-Larrondo, J., McDonald, M., Benson, B. A., et al. 2015, ApJ, 805, 35
Hudson, D. S., Mittal, R., Reiprich, T. H., et al. 2010, A&A, 513, A37
Kennicutt, R. C. 1998, ARA&A, 36, 189
Lau, E. T., Gaspari, M., Nagai, D., et al. 2017, ApJ, 849, 54.
Mantz, A. B., Allen, S. W., Morris, R. G., et al. 2015, MNRAS, 449, 199
McDonald, M., Veilleux, S., & Mushotzky, R. 2011, ApJ, 731, 33
McDonald, M., Bayliss, M., Benson, B. A., et al. 2012, Nature, 488, 349
McDonald, M., Benson, B. A., Vikhlinin, A., et al. 2013, ApJ, 774, 23
McDonald, M., Stalder, B., Bayliss, M., et al. 2016, ApJ, 817, 86
McDonald, M., Allen, S., Bayliss, M., et al. 2017, ApJ, 843, 28
McDonald, M., Gaspari, M., McNamara, B. R., et al. 2018, ApJ, 858, 45
McDonald, M., McNamara, B. R., Voit, G. M., et al. 2019, ApJ, 885, 63
McNamara, B. R., Rafferty, D. A., Bîrzan, L., et al. 2006, ApJ, 648, 164
McNamara, B. R. & Nulsen, P. E. J. 2012, New Journal of Physics, 14, 055023
Menanteau, F., Hughes, J. P., Sifón, C., et al. 2012, ApJ, 748, 7
Molendi, S., Tozzi, P., Gaspari, M., et al. 2016, A&A, 595, A123.
Panagoulia, E. K., Fabian, A. C., & Sanders, J. S. 2014, MNRAS, 438, 2341
Poole, G. B., Babul, A., McCarthy, I. G., et al. 2008, MNRAS, 391, 1163
Rafferty, D. A., McNamara, B. R., & Nulsen, P. E. J. 2008, ApJ, 687, 899
Somboonpanyakul, T., McDonald, M., Lin, H. W., et al. 2018, ApJ, 863, 122
Sun, M. 2009, ApJ, 704, 1586
Tonry, J. L., Stubbs, C. W., Lykke, K. R., et al. 2012, ApJ, 750, 99
Tremblay, G. R., O'Dea, C. P., Baum, S. A., et al. 2015, MNRAS, 451, 3768
Vikhlinin, A., Kravtsov, A., Forman, W., et al. 2006, ApJ, 640, 691
Voit, G. M., Donahue, M., Bryan, G. L., et al. 2015, Nature, 519, 203
Voit, G. M., Meece, G., Li, Y., et al. 2017, ApJ, 845, 80.
Voit, G. M. 2018, ApJ, 868, 102.
Wright, E. L., Eisenhardt, P. R. M., Mainzer, A. K., et al. 2010, AJ, 140, 1868